

1 **Flawed Emergency Intervention:**
2 **Slow Ocean Response**
3 **to Abrupt Stratospheric Aerosol Injection**

4 **Daniel Pflüger¹, Claudia E. Wieners¹, Leo van Kampenhout¹, René R.**
5 **Wijngaard¹, Henk A. Dijkstra¹**

6 ¹Institute Marine and Atmospheric Research Utrecht, Princetonplein 5, 3584 CC Utrecht, The
7 Netherlands

8 **Key Points:**

- 9
- 10 • Efficacy of SAI impaired by anthropogenic ocean heating
 - 11 • Deep ocean heating, weakened AMOC and collapsed North Atlantic deep convec-
12 tion only partially addressed by late SAI
 - 13 • SAI decouples AMOC and GMST, thereby inducing climate states not seen in purely
GHG-forced scenarios

Corresponding author: Daniel Pflüger, d.pfluger@uu.nl

Abstract

Given the possibility of irreversible, anthropogenic changes in the climate system, technologies such as solar radiation management (SRM) are sometimes framed as possible emergency interventions. However, little knowledge exists on the efficacy of such deployments. To fill in this gap, we perform Community Earth System Model 2 (CESM 2) simulations of an intense warming scenario on which we impose gradual early-century SRM or rapid late-century cooling (an emergency intervention), both realised via stratospheric aerosol injection (SAI). While both scenarios cool Earth's surface, ocean responses differ drastically. Rapid cooling fails to release deep ocean heat content or restore an ailing North Atlantic deep convection but partially stabilizes the Atlantic meridional overturning circulation. In contrast, the early intervention effectively mitigates changes in all of these features. Our results suggest that slow ocean timescales impair the efficacy of some SAI emergency interventions.

Plain Language Summary

Stratospheric aerosol injection (SAI) is a promising, yet controversial proposal to mask the effects of anthropogenic climate change by releasing sunlight-reflecting particles into the atmosphere. Currently, many studies are focusing on the benefits of near future SAI deployments. We, however, investigate SAI as a late *emergency intervention*. To what extent can SAI still help if we continue to heat and destabilize the climate?

In this study, we simulate the impacts of an abrupt, SAI cooling intervention deployed against the backdrop of a climate much hotter than today's. While SAI readily cools Earth's surface, it is challenged by a slow ocean response. Heat trapped below the ocean surface remains a contributor to sea-level rise and important currents weakened by climate change linger in ailing condition. In contrast, an earlier SAI intervention effectively mitigates changes in these features.

Our findings re-emphasize the urgent need for climate action. If anthropogenic heating continues, even an intervention as powerful as SAI will encounter its limits.

1 Introduction

While global heating puts increasing pressure on societies and ecosystems (IPCC, 2022a), current policies are insufficient to prevent 1.5°C or even 2°C of warming (IPCC, 2022b). To mitigate the associated risks, interventions that cool Earth by reflecting sunlight - *Solar Radiation Management* (SRM) - are being explored as complementary measures to emission reductions (National Academies of Sciences, Engineering, and Medicine, 2021). Among several potential schemes, *Stratospheric Aerosol Injection* (SAI) received considerable attention due to its low perceived technical barriers (Smith, 2020), plausible physical effectiveness (Kleinschmitt et al., 2018; Plazzotta et al., 2018). While model studies demonstrate its benefits (Tilmes et al., 2018, 2020; Vioni et al., 2021), including its ability to control global mean surface temperature (GMST), SAI can not address all consequences of rising greenhouse gas (GHG) concentrations and may induce side-effects of its own (Irvine et al., 2016; Zarnetske et al., 2021). Ethical concerns (Svoboda, 2017; Oomen, 2021) lead some to suggest a ban on its research and deployment (Biermann et al., 2022) whereas others suggest further research (Wieners et al., 2023).

It is not enough to ask *whether* SRM should be deployed. Multiple degrees of freedom in SRM deployments implore us to ask *how and to what end* may be SRM used. Currently popular frameworks include *peak-shaving* (Long & Shepherd, 2014; Reynolds, 2019), in which SRM stabilizes GMST, while other measures gradually tackle GHG concentrations. However, there is no guarantee SRM would be deployed in such a well-optimized and *proactive* fashion. In this study, we examine as SRM as an *emergency* intervention

62 instead, to be deployed only after prolonged heating. This notion, adapted from Lockley
 63 et al. (2022), naturally arises when SRM deployments are restricted to particularly ex-
 64 treme situations such as rapid climate tipping. To what extent can later deployments
 65 reverse the impacts of heating? How would they compare to earlier, proactive interven-
 66 tions?

67 In this study, we focus on SRM’s physical impact on the ocean. There, long response
 68 timescales hamper prospects of reversibility under an emergency intervention. Many ocean
 69 features are subject to anthropogenic climate change and have profound impacts on hu-
 70 mans and ecosystems which elevates the study of them above a purely academic exer-
 71 cise. We are interested in

- 72 • ocean heat content (OHC) change, a major contributor to sea-level rise (Church
 73 et al., 2013).
- 74 • the Atlantic Meridional Overturning Circulation (AMOC) which may weaken (or
 75 even collapse) in the future (Weijer et al., 2020), thereby reducing meridional heat
 76 transport and modulating regional sea level rise.
- 77 • North Atlantic deep convection which may shut down in the future, leading to abrupt
 78 cooling and shifts in the jet-stream (Sgubin et al., 2017; Swingedouw et al., 2021).

79 We consider only SRM scenarios with extreme levels of GHG and aerosol forcing,
 80 including abrupt changes thereof. They should not be seen as desirable or politically re-
 81 alistic futures but rather as physical edge cases that provide valuable intuitions and con-
 82 straints for more cautious scenarios: if an abrupt cooling struggles to reverse certain ocean
 83 changes, a slower deployment would likely do so, too. Furthermore, we restrict ourselves
 84 to a single SRM implementation: planetary-scale SAI.

85 2 Methods

86 Our scenarios are simulated in CESM2 (Danabasoglu et al., 2020) with atmospheric
 87 component CAM6 at $1^\circ \times 1^\circ$ horizontal resolution and ocean model POP2 at similar res-
 88 olution. Ice sheets are non-evolving, which also prohibits calving, but the land model CLM
 89 provides glacial run-off fluxes.

90 SAI is implemented via prescribed aerosol fields: a compromise between physical
 91 realism and computational cost. We favored this approach as it may enable computa-
 92 tionally cheap simulations capturing longer ocean timescales in the future. Other groups
 93 have used similar scaling-based implementations (Visioni et al., 2021).

94 Schematically, the protocol works as follows:

- 95 • Every year, observe the deviation of GMST from the target
- 96 • Based on past GMST deviations, infer the level of SAI - expressed in terms of global
 97 mean aerosol optical depth (AOD) - which is necessary to achieve the desired tar-
 98 get.
- 99 • Use the AOD to scale all SAI-related aerosol fields appropriately.
- 100 • Feed the scaled fields into CAM6.

101 The first two steps are implemented via an established feedforward-feedback con-
 102 trol algorithm (Kravitz et al., 2016, 2017). Our specific implementation stabilizes GMST
 103 as its sole objective, whereas interactive aerosol simulations (MacMartin et al., 2017; Tilmes
 104 et al., 2020) can also control other features such as the inter-hemispheric temperature
 105 contrast.

106 The input aerosol fields derive from an interactive aerosol simulation performed by
 107 Tilmes et al. (2020) in CESM2-WACCM, more specifically their Geo SSP5 8.5 1.5 sce-

108 nario. In contrast to CAM6, the improved, albeit more costly, atmospheric component
 109 WACCM allows for detailed chemical aerosol dynamics (Danabasoglu et al., 2020). Our
 110 prescribed aerosol fields are averaged versions of the WACCM aerosol fields as described
 111 in the supplementary material.

112 We simulate three scenarios based on SSP5-8.5 background concentrations:

- 113 • Control (2015-2100): historical spin-up continued by SSP5-8.5
- 114 • SAI2020 (gradual SAI): branch off Control in 2020; stabilise GMST at 1.5°C above
 115 pre-industrial conditions; analogous to Geo SSP5-8.5 1.5 by Tilmes et al. (2020)
- 116 • SAI2080 (emergency intervention): branch off Control in 2080, deploy SAI to re-
 117 store GMST to 1.5°C.

118 Note that SAI2080 involves some adjustments to the control algorithm, described
 119 in the supplementary material. Otherwise, the initially high deviation from the target
 120 GMST can overcharge the feedback controller and risk excessive cooling.

121 3 Results

122 3.1 Temperature Response

123 In Fig. 1A, we see that the gradual SAI strategy (SAI2020) indeed stabilises GMST
 124 at target level. By contrast, SAI2080 experiences rapid cooling and even shoots past the
 125 target. This undercooling is an artefact of the feedback controller and can be removed
 126 by fine-tuning the cooling process (Fig. S2).

127 Even though GMST is stabilised, total depth OHC accumulates continuously in
 128 SAI2020 (Fig.1B) in agreement with past studies (Fasullo et al., 2018; MacMartin et al.,
 129 2022). The warming takes place below the surface and likely stems from deep ocean re-
 130 sponse timescales (Cheng et al., 2022) combined with the goal of maintaining GMST.
 131 As sub-surface layers have not yet adapted to increased surface temperatures, they act
 132 as a heat sink for the ocean surface. The induced downward heat flux is then compen-
 133 sated by the feedback controller that allows for a residual top-of-atmosphere radiative
 134 imbalance in order to stabilize GMST.

135 SAI2080 accumulates more total depth OHC than SAI2020. The deep tail of OHC
 136 in SAI2080 (Fig.1C) matches that of Control while the near-surface layers are cooled
 137 to SAI2020 levels. Given the short time-frame of SAI2080, it is not clear whether the
 138 vertical OHC distribution has reached equilibrium or deeper layers are simply cooling
 139 very slowly.

140 On the surface, however, both SAI scenarios have comparable OHC anomalies. This
 141 suggests that while abrupt SAI readily cools the ocean surface, heat anomalies trapped
 142 in deeper layers are more persistent.

143 Surface temperature responses to SAI are spatially inhomogeneous (Fig. 2). Most
 144 strikingly, the subpolar North Atlantic is significantly undercooled in both SAI scenar-
 145 ios. This pattern resembles a *North Atlantic warming hole* known from purely GHG-forced
 146 simulations (Drijfhout et al., 2012; Menary & Wood, 2018), which to some extent is also
 147 visible in Control. SAI may have merely unmasked this feature rather than induce it.
 148 The warming hole is expanded and colder in SAI2080, while the Southern Hemisphere
 149 is warm compared to SAI2020.

150 Multi-objective feedback procedures (Kravitz et al., 2017; MacMartin et al., 2017)
 151 allow for a more elaborate control of the global temperature pattern including the in-
 152 terhemispheric temperature gradient. Therefore, the asymmetric response of SAI2080
 153 (Fig. 2E) may be mitigated in a refined control scheme. In our study, however, both SAI

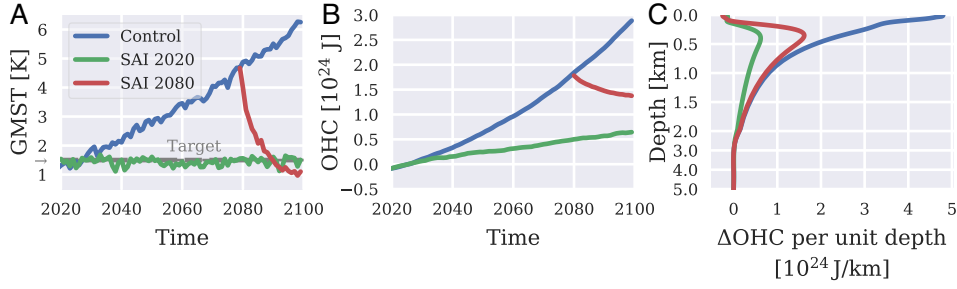


Figure 1. **A:** Annual mean GMST above pre-industrial reference temperature **B:** Change in annual mean total depth OHC relative to 2020-2030 conditions in Control. **C:** Difference in vertical OHC between end-of-simulation (2090-2100) conditions and present-day conditions in Control.

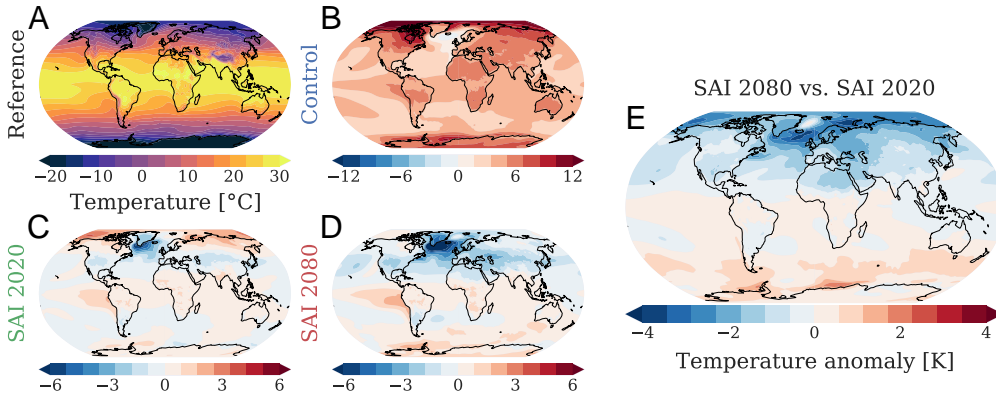


Figure 2. **A:** Reference (2020-2030) annual mean near-surface air temperatures in Control **B-D:** Late-century (2090-2100) temperature changes with respect to the reference for Control, SAI 2020 and SAI 2080 respectively. **E:** Difference between SAI scenarios (**D** minus **C**)

154 scenarios use spatially identical aerosol patterns which rules out a control of the asym-
 155 metry.

156 **3.2 AMOC Response**

157 The AMOC index and meridional heat transport (MHT) roughly halve in Control
 158 (Fig. 3A-B). Even the low-emission SSP1-2.6 scenario is projected to lead to similar AMOC
 159 index changes. SAI2020 drastically mitigates but does not halt the AMOC and MHT
 160 decline, similar to other studies (Xie et al., 2022; MacMartin et al., 2022). SAI 2080 sta-
 161 bilizes the AMOC index but only has an inconclusive impact on the MHT.

162 SAI effectively decouples the GMST and the AMOC index (Fig. 3C). This could
 163 explain the interhemispheric temperature contrast featured in SAI2080: a weak AMOC
 164 impedes northward heat transport leading to a see-saw temperature pattern (Stocker,
 165 1998; Liu et al., 2020) not masked by heat otherwise present in Control.

166 To study the spatial pattern of the AMOC, we plot meridional streamfunction changes
 167 under all scenarios from 2070-2080 to 2090-2100 (Fig. 4). This choice of time intervals
 168 helps to reveal the immediate AMOC response to SAI 2080. Additionally, we subtract

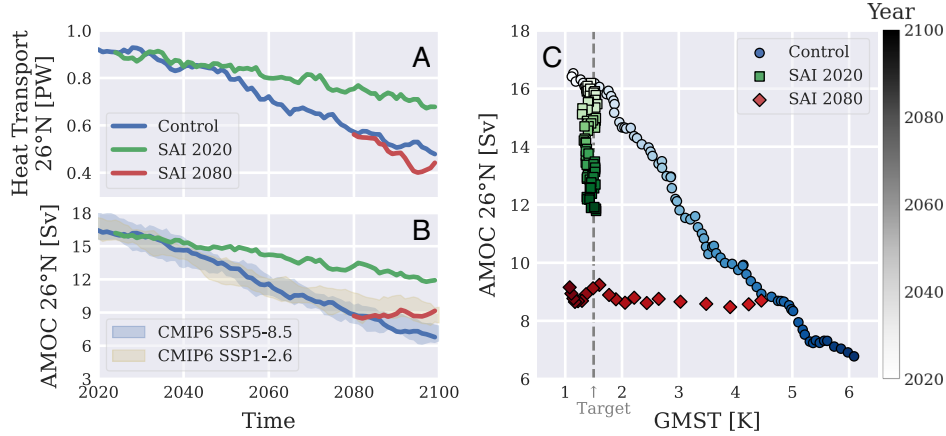


Figure 3. **A:** Annual mean Atlantic northwards heat transport at 26°N where we apply a rolling average over five year periods with backward window **B:** AMOC index defined as the maximum of the annual mean meridional overturning streamfunction at 26°N below 200 m - Partially transparent uncertainty bands depict three CESM2 CMIP6 (Coupled Model Intercomparison Project Phase 6) ensemble members (Danabasoglu, 2019c, 2019d) per GHG concentration pathway. The uncertainty is the ensemble standard deviation. Again, we apply rolling averages over five year periods. **C:** Annual mean GMST vs. AMOC index - The marker saturation denotes the year: light (2020) to dark (2100).

169 the changes in Control from the ones in the SAI scenarios in an attempt to disentangle
 170 GHG from SAI-related impacts.

171 Fig. 4D reveals a potential feedback in the AMOC stabilization under SAI2080. Fol-
 172 lowing the deployment, the pattern of relative AMOC strengthening closely mirrors the
 173 pre-deployment streamfunction, albeit mostly near the surface and in the northern hemi-
 174 sphere. This suggests that the AMOC response to abrupt SAI is dependent on the AMOC
 175 state itself. While a similar observation can be made for SAI2020 (Fig. 4C), disen-
 176 tangleing the forced response from internal feedback is not obvious during the gradual
 177 change in aerosol forcing. SAI2080 gives a much better indication that it is indeed the state of
 178 the AMOC which steers its response to SAI.

179 **3.3 North Atlantic Deep Convection**

180 We now focus on deep convection processes in the North Atlantic. Using mixed layer
 181 depth as a proxy for deep convection, we identify two regions, *East* and *West*, where the
 182 mixed layer depth in April (the month with the deepest mixed layer) exceeds 550 m (Fig. 5A).
 183 This threshold depth was chosen as it is sufficiently large to distinguish deep convection
 184 from regular mixed-layer conditions and small enough to provide a good signal-to-noise
 185 ratio. The regions are separated longitudinally by the southern tip of Greenland.

186 In Control, deep convection in *West* ceases around 2050, followed by a shutdown
 187 in *East* around 2060. SAI2020 prevents the shutdown in *East*, but only postpones the
 188 shutdown in *West* by about a decade. The *West* shutdown is not as definite as in the
 189 case of Control and isolated years with deep convection still occur. For SAI2080, deep
 190 convection remains absent in both regions with the exception of a single outlier year for
 191 *East*.

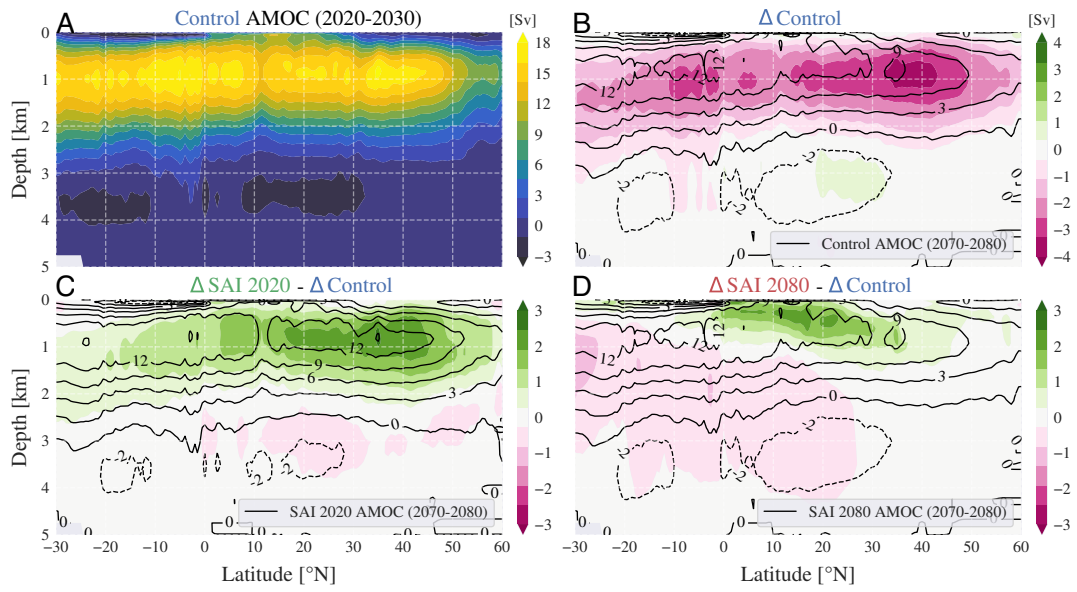


Figure 4. **A:** AMOC streamfunction in Control averaged over 2020-2030. In **B-D**, for any simulation X, ΔX is the mean over 2090-2100 minus the mean over 2070-2080. **B:** Change in AMOC streamfunction under Control - Black contour lines show the mean streamfunction over 2070-2080 for Control while the shading indicates Δ Control. **C:** Change in AMOC streamfunction in SAI2020 relative to Control - Black contour lines show the mean streamfunction over 2070-2080 for SAI2020 while the shading indicates Δ SAI 2020 - Δ Control. **D:** Analogous to **C** but for SAI2080.

192 Why does cooling in SAI2080 not revive deep convection before 2100? We address
 193 this question by studying the ocean stratification over both deep convection regions. Deep
 194 convection in April is inhibited if the surface density in the previous September has been
 195 too low, i.e. the water column was too stratified (Fig. S4). Thus, surface density serves
 196 as a proxy for favorable convection conditions.

197 The sea surface density is determined by temperature and salinity, seen in Fig. 5D-
 198 F. In all scenarios, final salinities are well below reference conditions. SAI2020 roughly
 199 halves the decline with respect to Control. This difference becomes very noticeable mid-
 200 century simultaneously with the *East* and *West* shutdown in Control. SAI2080 does not
 201 fundamentally alter the trajectory of Control apart from a transient increase in salin-
 202 ity that correlates with an isolated year of deep convection. Therefore, freshening con-
 203 tributes to density loss in all scenarios.

204 In the case of Control, temperature trends are non-monotonous (Fig. 5D) and do
 205 not lead to a denser surface. What appears to be a weak cooling trend is mostly masked
 206 by inter-annual variability and eventually superseded by intense heating. Typically, deep
 207 convection shutdown induces a rapid cooling (Sgubin et al., 2017; Swingedouw et al., 2021)
 208 which is not obvious from Fig. 5D. It can, however, be detected by using a CESM2 SSP5-
 209 8.5 ensemble and switching to an annual-mean rather than a single-month perspective
 210 (Fig. S6).

211 SAI2020 shows an overall cooling trend dominated by a quick decline at time of
 212 *West* shutdown. Former observation could indicate AMOC weakening whereas latter phe-
 213 nomenon is again consistent with abrupt cooling during deep convection collapse (Sgubin
 214 et al., 2017; Swingedouw et al., 2021). In SAI2080, the cooling is more drastic (Fig. 5D),
 215 perhaps a result of full deep convection shutdown and a weakened AMOC. These tem-
 216 perature drops have a positive effect on density and thereby convection, albeit not suf-
 217 ficient to bring SAI2080 densities to SAI2020 levels (Fig. 5F). Therefore, the salinity deficit
 218 of SAI2080 with respect to SAI2020 (Fig. 5E) presents a clear obstacle to restarting deep
 219 convection.

220 Recognizing the importance of salinity changes, we sketch a possible mechanism
 221 behind SAI2080's failure to spur convection. Firstly, all scenarios see an increase in sur-
 222 face freshwater forcing (Fig. S3) which contributes to a gradual salinity loss. This weak-
 223 ens convection and consequently the AMOC. Subsequently, weak AMOC and convec-
 224 tion reduce salt transport into the subpolar gyre reinforcing the salinity decline (Kuhlbrodt
 225 et al., 2007). While SAI2020 mitigates these feedbacks early on, SAI2080 arrives only
 226 after substantial freshening. Closing the density gap via cooling then runs into 'dimin-
 227 ishing returns': density gains are less than proportional to temperature decreases (Fig. S5).

228 Another potentially important factor not included in this analysis is Greenland run-
 229 off. It likely contributes to fresher subpolar gyre conditions in SAI2080. Additionally,
 230 Arctic outflows also supply freshwater to the deep convection regions and could vary de-
 231 pending on the scenario (Li et al., 2021).

232 4 Discussion

233 In our simulations, the quick drop in GMST due to abrupt SAI is contrasted by
 234 a slow ocean response. Gradual early-century SAI, on the other hand, retains an ocean
 235 state much closer to the present-day reference. Elevated OHC, weak AMOC and absent
 236 deep convection coupled with a lower GMST presents a (transient) climate state unknown
 237 from purely GHG-forced scenarios.

238 Note that our scenarios are extreme cases with a high signal-to-noise ratio, rather
 239 than desirable or plausible futures. More cautious protocols typically deploy SAI in tan-
 240 dem with emission mitigation to limit a temporary temperature overshoot (National Academies

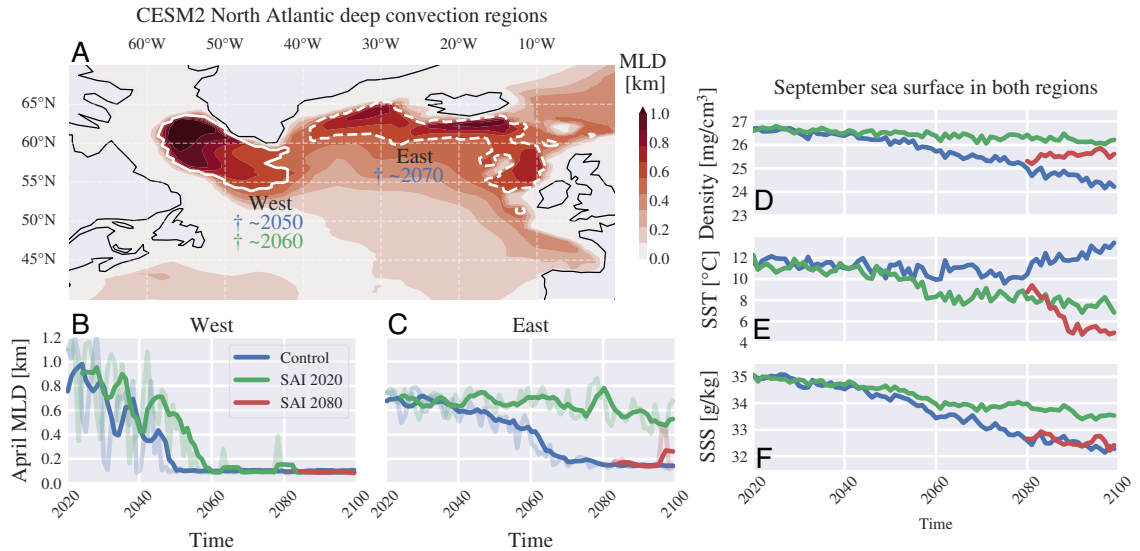


Figure 5. **A:** North Atlantic April mixed layer depths in CESM2 (2020-2030) - *East* and *West* are enclosed by solid and dashed lines respectively. Shutdown dates are denoted with a cross and colored according to scenario (blue: Control, green: SAI 2020). **B-C:** April mixed layer depths in *West* and *East* respectively - Solid lines are five year rolling means (with backward window) applied to the data shown by transparent lines. **D-F:** September mean sea surface density, temperature and salinity over the total *East* and *West* region

241 of Sciences, Engineering, and Medicine, 2021). If a cooling scenario were actually con-
 242 sidered, a ramp-up of SAI would be more sensible than the sudden deployment in SAI 2080.
 243 Such a gradual approach would enable a fine-tuning of the injection scheme based on ob-
 244 servations.

245 Besides the high forcings, our scenarios also involve a limited SAI scheme. As our
 246 implementation relies on a single degree of freedom, we can only meet a GMST target
 247 but not control other aspects of the temperature pattern. More control parameters, on
 248 the other hand, may be beneficial to prevent a interhemispheric temperature asymme-
 249 try which risks a displacement of the ITCZ (Broccoli et al., 2006; Bischoff & Schneider,
 250 2016). Still, restoring the meridional temperature pattern in SAI2080 would come with
 251 problems of its own: less cooling over the North Atlantic further endangers deep con-
 252 vection.

253 As for our results, a mitigating effect of SAI on AMOC decline was already known
 254 in multiple models and scenarios (Tilmes et al., 2018, 2020; Xie et al., 2022; MacMartin
 255 et al., 2022) but not in the case of late-century abrupt deployment. To our knowledge,
 256 no studies have been performed on the effect of SAI on deep convection shutdown either.
 257 Model dependencies are certain as deep convection shutdown is not a universal phenomenon
 258 in CMIP6 (Swingedouw et al., 2021). In fact, the absence of a warming hole in another
 259 SAI study using the UKESM1 model (Henry et al., 2023) could indicate a deep convec-
 260 tion more stable than that of CESM2.

261 It is worth pointing out similarities between our abrupt SAI case and rapid nega-
 262 tive emission scenarios (Schwinger et al., 2022). Removal of GHG after prolonged heat-
 263 ing can lead to an interhemispheric temperature asymmetry if the timescale of extrac-
 264 tion is shorter than that of the AMOC recovery. Therefore, the possibility of SAI to man-

265 age the interhemispheric temperature gradient is an advantage compared to GHG re-
266 moval.

267 A major questions remains open: do the climates of both SAI scenarios eventually
268 converge? This question cannot be answered without extending the simulations, which
269 is outside the scope of this study. When extrapolating our results, the OHC difference
270 is expected to lessen due to residual ocean warming in SAI2020. Whether the gap fully
271 closes may also depend on the AMOC and deep convection because of their impact on
272 ocean heat uptake (Marshall & Zanna, 2014). As for deep convection, the aforementioned
273 salinity deficit in SAI2080 inhibits convergence of the SAI scenarios. Nevertheless, should
274 some years of deep convection arise in SAI2080 (e.g. as a result of natural variability),
275 salt import would be strengthened, thereby improving long-term prospects of a revival.

276 **5 Summary**

277 In this study, we presented model results of a late-century SAI emergency inter-
278 vention that aims to restore surface temperatures under simultaneous GHG forcing. By
279 comparing our findings with a gradual early-century SAI scenario, we show that abrupt
280 late-century SAI is less effective at mitigating changes in OHC, the AMOC and North
281 Atlantic deep convection.

282 Firstly, abrupt SAI failed to release heat trapped in deeper ocean layers. Even an
283 early onset of SAI only mitigates but does not halt OHC accumulation. Both results are
284 linked to slow ocean equilibration times and the target of GMST stabilization.

285 Secondly, abrupt SAI partially stabilized a weakened AMOC, albeit not halting the
286 decline of northward heat transport. Under earlier SAI, the AMOC decline is mitigated
287 in both, volume and heat transport. As a result, the scenarios reach drastically differ-
288 ent AMOC states despite comparable GMST. A weaker AMOC may contribute to the
289 observed undercooling of the northern hemisphere in the emergency intervention scenario.
290 This, in turn, may be relevant for the choice of injection pattern.

291 Thirdly, a shutdown of North Atlantic deep convection could not be reversed with
292 rapid, SAI-induced cooling. We suspect that a weakened AMOC, absence of convective
293 feedback, fresher surface conditions and a sub-proportional density response of water to
294 cooling pose an obstacle for restarting deep convection. An early intervention, on the
295 other hand, retains more salt in the North Atlantic, hence the partial stabilization of deep
296 convection.

297 Our findings reveal limitations of an SAI emergency deployment: reversing ocean
298 changes after they occur is less feasible than preventing them in the first place. In this
299 context, proactive SAI deployments may be beneficial. Delaying climate action - this in-
300 cludes emission mitigation - in the hope of a later rescue through SAI will come at a price.

301 **6 Open Research**

302 Our CESM2-CAM6 SAI implementation (Pflüger, 2023b), including the input aerosol
303 fields we used, analysis tools (Pflüger, 2023a) and the notebooks used to generate fig-
304 ures (Pflüger, 2023c) can be found on public GitHub repositories. The simulation out-
305 put required to create all figures is stored in a Zenodo repository (Pflüger et al., 2024).
306 More simulation data can be made available upon reasonable request. The CMIP6 data
307 used for comparison in Fig. 3 is publicly available (Danabasoglu, 2019c, 2019d).

308 **Acknowledgments**

We thank Daniele Visionsi, Doug MacMartin and Ben Kravitz for sharing their feedback controller code, our colleague Michael Kliphuis for providing his AMOC stream-function tools and Simone Tilmes for providing CESM2-WACCM data. Furthermore, we thank Jasper de Jong and Michiel Baatsen for fruitful discussions on the feedback control of SAI2080.

References

- Astrom, K. J., & Rundqwist, L. (1989). Integrator windup and how to avoid it. In *1989 American Control Conference*.
- Biermann, F., Oomen, J., Gupta, A., Ali, S. H., Conca, K., Hajer, M. A., ... Van-Deveer, S. D. (2022). Solar geoengineering: The case for an international non-use agreement. *WIREs Climate Change*. doi: 10.1002/wcc.754
- Bischoff, T., & Schneider, T. (2016). The equatorial energy balance, ITCZ position, and double-ITCZ bifurcations. *Journal of Climate*. doi: 10.1175/JCLI-D-15-0328.1
- Broccoli, A. J., Dahl, K. A., & Stouffer, R. J. (2006). Response of the ITCZ to northern hemisphere cooling. *Geophysical Research Letters*. doi: 10.1029/2005GL024546
- Cheng, L., Von Schuckmann, K., Abraham, J. P., Trenberth, K. E., Mann, M. E., Zanna, L., ... Lin, X. (2022). Past and future ocean warming. *Nature Reviews Earth & Environment*. doi: 10.1038/s43017-022-00345-1
- Church, J. A., White, N. J., Domingues, C. M., Monselesan, D. P., & Miles, E. R. (2013). Sea-level and ocean heat-content change. In *International geophysics* (Vol. 103, pp. 697–725). Elsevier. Retrieved from <https://linkinghub.elsevier.com/retrieve/pii/B9780123918512000271> doi: 10.1016/B978-0-12-391851-2.00027-1
- Danabasoglu, G. (2019a). *NCAR CESM2 model output prepared for CMIP6 ScenarioMIP ssp126* [Dataset]. <http://dx.doi.org/10.22033/ESGF/CMIP6.7746>. Earth System Grid Federation.
- Danabasoglu, G. (2019b). *NCAR CESM2 model output prepared for CMIP6 ScenarioMIP ssp245* [Dataset]. <http://dx.doi.org/10.22033/ESGF/CMIP6.7748>. Earth System Grid Federation.
- Danabasoglu, G. (2019c). *NCAR CESM2 model output prepared for CMIP6 ScenarioMIP ssp370* [Dataset]. Earth System Grid Federation. doi: 10.22033/ESGF/CMIP6.7753
- Danabasoglu, G. (2019d). *NCAR CESM2 model output prepared for CMIP6 ScenarioMIP ssp585* [Dataset]. Earth System Grid Federation. doi: 10.22033/ESGF/CMIP6.7768
- Danabasoglu, G., Lamarque, J., Bacmeister, J., Bailey, D. A., DuVivier, A. K., Edwards, J., ... Strand, W. G. (2020). The community earth system model version 2 (CESM2). *Journal of Advances in Modeling Earth Systems*. doi: 10.1029/2019MS001916
- Drijfhout, S., van Oldenborgh, G. J., & Cimadoribus, A. (2012). Is a decline of AMOC causing the warming hole above the north atlantic in observed and modeled warming patterns? *Journal of Climate*. doi: 10.1175/JCLI-D-12-00490.1
- Fasullo, J. T., Tilmes, S., Richter, J. H., Kravitz, B., MacMartin, D. G., Mills, M. J., & Simpson, I. R. (2018). Persistent polar ocean warming in a strategically geoengineered climate. *Nature Geoscience*. doi: 10.1038/s41561-018-0249-7
- Hansen, J., Sato, M., Ruedy, R., Nazarenko, L., Lacis, A., Schmidt, G., ... others (2005). Efficacy of climate forcings. *Journal of Geophysical Research: Atmospheres*.
- Henry, M., Haywood, J., Jones, A., Dalvi, M., Wells, A., Visionsi, D., ... Tye, M. R.

- (2023). Comparison of UKESM1 and CESM2 simulations using the same multi-target stratospheric aerosol injection strategy. *Atmospheric Chemistry and Physics*, 23(20), 13369–13385. doi: 10.5194/acp-23-13369-2023
- IPCC. (2022a). *Climate change 2022: Impacts, adaptation and vulnerability*. Cambridge University Press. doi: 10.1017/9781009325844
- IPCC. (2022b). *Climate change 2022: Mitigation of climate change*. Cambridge University Press.
- Irvine, P. J., Kravitz, B., Lawrence, M. G., & Muri, H. (2016). An overview of the earth system science of solar geoengineering. *WIREs Climate Change*, 7(6), 815–833. doi: 10.1002/wcc.423
- Kleinschmitt, C., Boucher, O., & Platt, U. (2018). Sensitivity of the radiative forcing by stratospheric sulfur geoengineering to the amount and strategy of the SO₂ injection studied with the LMDZ-S3A model. *Atmospheric Chemistry and Physics*. doi: 10.5194/acp-18-2769-2018
- Kravitz, B., MacMartin, D. G., Mills, M. J., Richter, J. H., Tilmes, S., Lamarque, J., ... Vitt, F. (2017). First simulations of designing stratospheric sulfate aerosol geoengineering to meet multiple simultaneous climate objectives. *Journal of Geophysical Research: Atmospheres*. doi: 10.1002/2017JD026874
- Kravitz, B., MacMartin, D. G., Wang, H., & Rasch, P. J. (2016). Geoengineering as a design problem. *Earth System Dynamics*. doi: 10.5194/esd-7-469-2016
- Kuhlbrodt, T., Griesel, A., Montoya, M., Levermann, A., Hofmann, M., & Rahmstorf, S. (2007). On the driving processes of the atlantic meridional overturning circulation. *Reviews of Geophysics*.
- Lawrence, D., Fisher, R., Koven, C., Oleson, K., Swenson, S., Vertenstein, M., et al. (2018, February). *Technical description of version 5.0 of the community land model (clm)* (Technical Report). National Center for Atmospheric Research. https://www2.cesm.ucar.edu/models/cesm2/land/CLM50_Tech_Note.pdf.
- Li, F., Lozier, M. S., Holliday, N. P., Johns, W. E., Le Bras, I. A., Moat, B. I., ... De Jong, M. F. (2021). Observation-based estimates of heat and freshwater exchanges from the subtropical north atlantic to the arctic. *Progress in Oceanography*, 197, 102640. doi: 10.1016/j.pocean.2021.102640
- Liu, W., Fedorov, A. V., Xie, S.-P., & Hu, S. (2020). Climate impacts of a weakened atlantic meridional overturning circulation in a warming climate. *Science Advances*. doi: 10.1126/sciadv.aaz4876
- Lockley, A., Xu, Y., Tilmes, S., Sugiyama, M., Rothman, D., & Hinds, A. (2022). 18 politically relevant solar geoengineering scenarios. *Socio-Environmental Systems Modelling*. doi: 10.18174/sesmo.18127
- Long, J. C. S., & Shepherd, J. G. (2014). The strategic value of geoengineering research. In B. Freedman (Ed.), *Global environmental change*. Springer Netherlands. doi: 10.1007/978-94-007-5784-4_24
- MacMartin, D. G., Kravitz, B., Tilmes, S., Richter, J. H., Mills, M. J., Lamarque, J., ... Vitt, F. (2017). The climate response to stratospheric aerosol geoengineering can be tailored using multiple injection locations. *Journal of Geophysical Research: Atmospheres*. doi: 10.1002/2017JD026868
- MacMartin, D. G., Visioni, D., Kravitz, B., Richter, J., Felgenhauer, T., Lee, W. R., ... Sugiyama, M. (2022). Scenarios for modeling solar radiation modification. *Proceedings of the National Academy of Sciences*. doi: 10.1073/pnas.2202230119
- Marshall, D. P., & Zanna, L. (2014). A conceptual model of ocean heat uptake under climate change. *Journal of Climate*. doi: 10.1175/JCLI-D-13-00344.1
- Menary, M. B., & Wood, R. A. (2018). An anatomy of the projected north atlantic warming hole in CMIP5 models. *Climate Dynamics*. doi: 10.1007/s00382-017-3793-8
- National Academies of Sciences, Engineering, and Medicine. (2021). *Reflecting sunlight: Recommendations for solar geoengineering research and research*

- 417 *governance*. National Academies Press. doi: 10.17226/25762
- 418 Oomen, J. (2021). *Imagining climate engineering: dreaming of the designer climate*.
419 Routledge, Taylor & Francis Group.
- 420 Pflüger, D. (2023a). *cesm_tools* [Software]. Retrieved 2023-12-11, from [https://](https://github.com/daniel-pflueger/cesm_tools)
421 github.com/daniel-pflueger/cesm_tools
- 422 Pflüger, D. (2023b). *imau_cesm2_prescribed_aerosols* [Software]. Retrieved 2023-
423 12-11, from [https://github.com/daniel-pflueger/imau_cesm2_prescribed](https://github.com/daniel-pflueger/imau_cesm2_prescribed_aerosols)
424 [_aerosols](https://github.com/daniel-pflueger/imau_cesm2_prescribed_aerosols)
- 425 Pflüger, D. (2023c). *sai_ocean_figures_2023* [Notebook]. Retrieved 2023-12-11, from
426 https://github.com/daniel-pflueger/sai_ocean_figures_2023
- 427 Pflüger, D., Wieners, C. E., van Kampenhout, L., Wijngaard, R. R., & Di-
428 jkstra, H. A. (2024). *Flawed emergency intervention: Slow ocean re-*
429 *sponse to abrupt stratospheric aerosol injection (Dataset)* [Dataset]. doi:
430 10.5281/zenodo.10606102
- 431 Plazzotta, M., Séférian, R., Douville, H., Kravitz, B., & Tjiputra, J. (2018). Land
432 surface cooling induced by sulfate geoengineering constrained by major vol-
433 canic eruptions. *Geophysical Research Letters*. doi: 10.1029/2018GL077583
- 434 Reynolds, J. L. (2019). Solar geoengineering to reduce climate change: a review of
435 governance proposals. *Proceedings of the Royal Society A: Mathematical, Phys-*
436 *ical and Engineering Sciences*(2229). doi: 10.1098/rspa.2019.0255
- 437 Schwinger, J., Asaadi, A., Goris, N., & Lee, H. (2022). Possibility for strong north-
438 ern hemisphere high-latitude cooling under negative emissions. *Nature Com-*
439 *munications*. doi: 10.1038/s41467-022-28573-5
- 440 Sgubin, G., Swingedouw, D., Drijfhout, S., Mary, Y., & Bennabi, A. (2017). Abrupt
441 cooling over the north atlantic in modern climate models. *Nature Communica-*
442 *tions*. doi: 10.1038/ncomms14375
- 443 Smith, W. (2020). The cost of stratospheric aerosol injection through 2100. *Environ-*
444 *mental Research Letters*. doi: 10.1088/1748-9326/aba7e7
- 445 Stocker, T. F. (1998). The seesaw effect. *Science*. doi: 10.1126/science.282.5386.61
- 446 Svoboda, T. (2017). *The ethics of climate engineering: solar radiation management*
447 *and non-ideal justice*. Routledge, Taylor & Francis Group.
- 448 Swingedouw, D., Bily, A., Esquerdo, C., Borchert, L. F., Sgubin, G., Mignot, J., &
449 Menary, M. (2021). On the risk of abrupt changes in the north atlantic subpo-
450 lar gyre in CMIP6 models. *Annals of the New York Academy of Sciences*. doi:
451 10.1111/nyas.14659
- 452 Tilmes, S., MacMartin, D. E., Lenaerts, J. T. M., Van Kampenhout, L., Muntjewerf,
453 L., Xia, L., . . . Robock, A. (2020). Reaching 1.5 °c and 2.0 °c global surface
454 temperature targets using stratospheric aerosol geoengineering. *Earth System*
455 *Dynamics*. doi: 10.5194/esd-11-579-2020
- 456 Tilmes, S., Richter, J. H., Kravitz, B., MacMartin, D. G., Mills, M. J., Simpson,
457 I. R., . . . Ghosh, S. (2018). CESM1(WACCM) stratospheric aerosol geo-
458 engineering large ensemble project. *Bulletin of the American Meteorological*
459 *Society*. doi: 10.1175/BAMS-D-17-0267.1
- 460 Visioni, D., MacMartin, D. G., Kravitz, B., Boucher, O., Jones, A., Lurton, T., . . .
461 Tilmes, S. (2021). Identifying the sources of uncertainty in climate model
462 simulations of solar radiation modification with the g6sulfur and g6solar geo-
463 engineering model intercomparison project (GeoMIP) simulations. *Atmospheric*
464 *Chemistry and Physics*, 21. doi: 10.5194/acp-21-10039-2021
- 465 Visioni, D., MacMartin, D. G., Kravitz, B., Lee, W., Simpson, I. R., & Richter,
466 J. H. (2020). Reduced poleward transport due to stratospheric heating un-
467 der stratospheric aerosols geoengineering. *Geophysical Research Letters*. doi:
468 10.1029/2020GL089470
- 469 Weijer, W., Cheng, W., Garuba, O. A., Hu, A., & Nadiga, B. T. (2020). CMIP6
470 models predict significant 21st century decline of the atlantic meridional
471 overturning circulation. *Geophysical Research Letters*. doi: 10.1029/

472 2019GL086075

- 473 Wieners, C. E., Hofbauer, B. P., De Vries, I. E., Honegger, M., Visionsi, D., Russ-
474 chenberg, H. W. J., & Felgenhauer, T. (2023). Solar radiation modification is
475 risky, but so is rejecting it: a call for balanced research. *Oxford Open Climate*
476 *Change*. doi: 10.1093/oxfclm/kgad002
- 477 Xie, M., Moore, J. C., Zhao, L., Wolovick, M., & Muri, H. (2022). Impacts of three
478 types of solar geoengineering on the atlantic meridional overturning circula-
479 tion. *Atmospheric Chemistry and Physics*. doi: 10.5194/acp-22-4581-2022
- 480 Zarnetske, P. L., Gurevitch, J., Franklin, J., Groffman, P. M., Harrison, C. S., Hell-
481 mann, J. J., . . . Yang, C.-E. (2021). Potential ecological impacts of climate
482 intervention by reflecting sunlight to cool earth. *Proceedings of the National*
483 *Academy of Sciences*. doi: 10.1073/pnas.1921854118